ORIGINAL ARTICLE

Geophysical investigation for shallow subsurface geotechnical problems of Mokattam area, Cairo, Egypt

Sultan Awad Sultan Araffa

Abstract Nine vertical electrical soundings of Schlumberger configuration were measured with $AB/2 = 1$–500 m. Manual and computerized interpretation were done to detect the subsurface stratigraphy of the study area. The results show that the subsurface section consists of alternated units of limestone, clay, marly limestone and dolomitic limestone and the thickness of clay unit ranged from 10 to 40 m. Nine dipole–dipole sections have also been constructed to give a clearer picture of the subsurface at the study area. The length of each dipole–dipole section is 235 m, with a electrode spacing ranging between 5 and 25 m. The Res2Dinv software was used for processing and interpretation of field data. The dipole–dipole sections at the upper plateau display high resistivity values at most parts of the plateau. Twelve shallow seismic refraction profiles are measured at selected locations for the dipole sections to define the interface between the fractured limestone and the upper surface of the clay layer. Each profile consists of 24 geophones with a geophone spacing of 2–3 m. Interpretation of seismic data indicates that the surface layer of the upper plateau consists of fractured limestone with a velocity range of 1.16–1.56 km/s and another layer of compacted clay with a velocity range of 1.38–1.88 km/s. Furthermore, the surface layer of the middle plateau consists of marl and marly limestone with a velocity about 2.1 km/s and its underlying layer consists of massive limestone with a velocity of 4.94 km/s.

Keywords Resistivity · Shallow seismic refraction · Fractures · Limestone · Clay

S. A. S. Araffa (✉)
National Research Institute of Astronomy and Geophysics,
Helwan, 11722 Cairo, Egypt
e-mail: sultan_awad@yahoo.com

Introduction

The study area is located at the eastern part of Cairo bounded by latitudes 29° 59′ 20″ and 30° 00′ 50″ and longitudes 31° 16′ 30″ and 31° 19′ (Fig. 1). Geomorphologically, the Mokattam area consists of three plateaus. The upper plateau lies at the northern part and has high elevation ranging from 205 m at the southern part to 170 m at the northern part and separated from the middle plateau by a steep cliff. The middle plateau has an elevation ranging from 110 to 150 m. The lower plateau has an elevation ranging from 50 to 80 m (NARSS 1997). Moustafa et al. (1985, 1991) and Moustafa and Abdel Twaab (1985) studied the engineering properties of the upper and middle plateaus of Gable Mokattam. The Geological survey of Egypt (EGSMA 2004) studied the foundation properties and structural framework of Mokattam area. Sultan et al. (2004) conducted a geoelectrical survey at two localities in Greater Cairo, Egypt. Also, Sultan et al. (2006) used the geoelectrical techniques to detect the groundwater seepage on Hibis temple, Kharaga, Egypt. The slopes of the Middle Eocene rocks which form the boundaries of the middle plateau of G. Mokattam are unstable and represent potential areas of rock failure in many places (Yousif 2000). The Mokattam plateau represents dangerous problems especially at the borders of the plateau, where at the southern part of the Mokattam plateau there have been many landslides due to the fractured limestone. The landslides caused damage to many houses and hotels. The fractured limestone is overlain by a clay layer which causes most engineering problems due to volume changes in swelling clays result from activities of man that modify the local environments (Velde 1995). Recently, in August 2008 big blocks of limestone fell on the urban area at the northern part of Mokattam plateaus, and 105 persons were died and 75 were wounded.

The present study aims to define the geotechnical problems, which arise from swelling of clays and natural caves in limestone, and also surveying for the clay layer which is source of many geotechnical problems at the upper plateau (Fig. 2).

Geology of the area

The surface geology of the study area was described by the Geological Survey of Egypt and the National Authority of Remote Sensing and Space Sciences (NARSS 1997) (Fig. 1). The area consists of two formations of Upper Eocene age. The first is the Maadi Formation which consists of soft clastic rocks (clay, silt and sand) and hard dolomitic limestone. The second formation is the Giushi Formation, which consists of white fossiliferous limestone with marl intercalation. The study area is dissected by different structural elements most of them have NWN–SES, E–W and NW–SE trends.

Fig. 1 Location and geological map of the study area (after NARSS 1997)
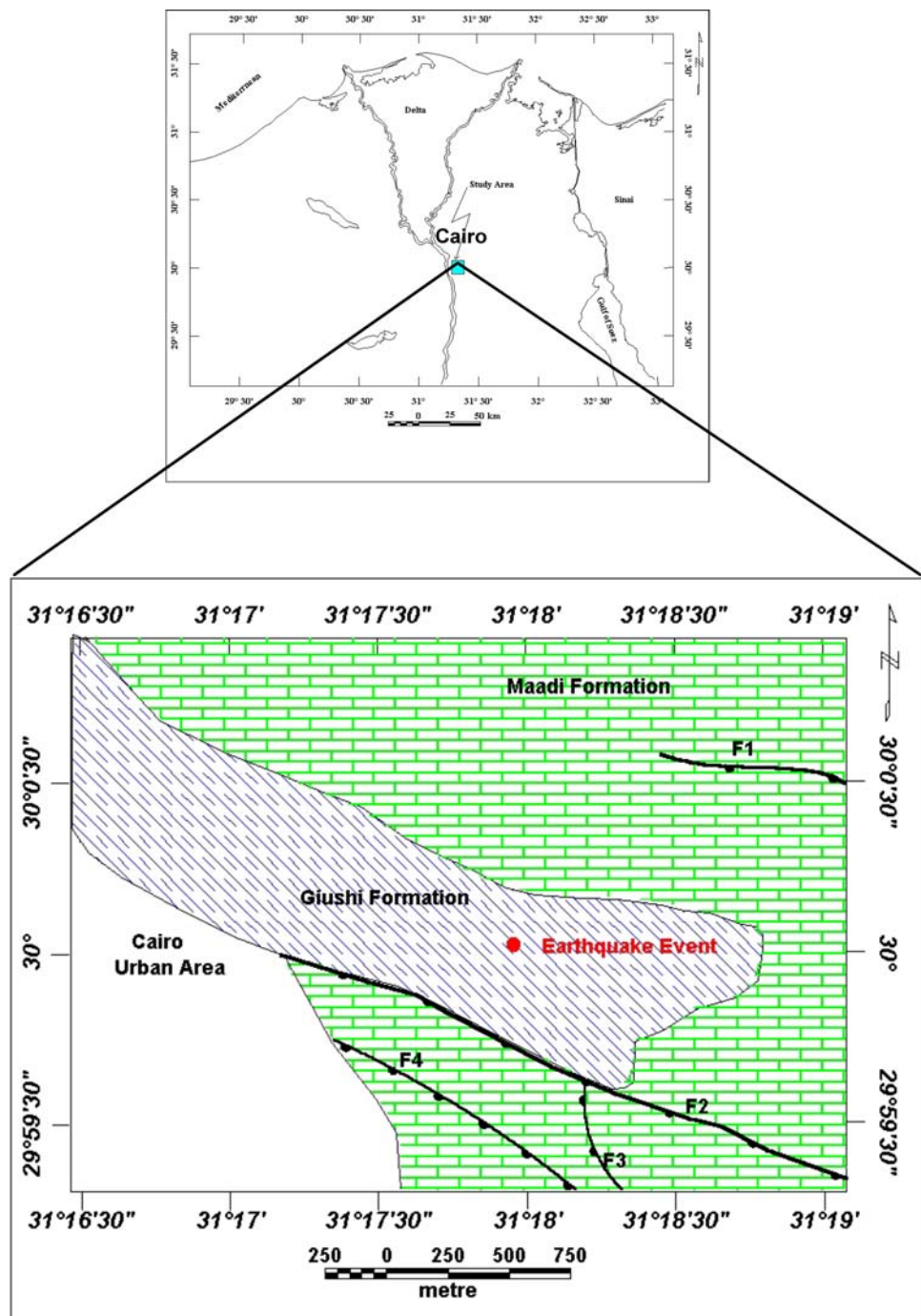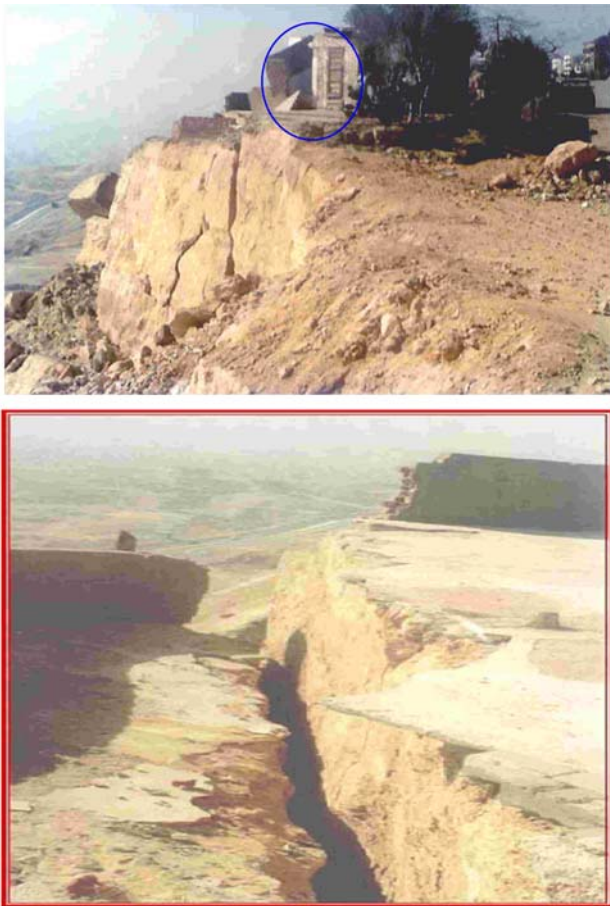
Fig. 2 Photos show the damage at the Mokattam hotel for the upper photo, fractures at limestone layer in the lower photo

The subsurface stratigraphy of Mokattam area is described through a borehole drilled by EGSMA (1994). The total depth of the borehole is 225 m, where the first 68 m represents the Maadi Formation which composed of fractured limestone and clay. The Giushi Formation is at the depths of from 68 to 112 m. The depth from 112 to 159.35 m represents the Upper building stone Member of Mokattam Formation, while the depth from 159.35 to 165.7 m represents the Gizahensis Member (Mokattam Formation). The depth from 165.7 m to the end of the borehole 225 m is represented by the lower building stone Member of Mokattam Formation.

Geophysical measurements and interpretation

Deep geophysical measurements (vertical electrical sounding)

The vertical electrical sounding (VES) carried out by measuring nine VES stations of electrode-separations ranging from $AB/2 = 1–500$ m using the Schlumberger

configuration over the southern part of the upper plateau and the middle plateau (Fig. 3a). Measurements were made by using a SYSCAL—R2, resistivity—meter, which can be connected to a network of intelligent nodes and to be used as an automatic Multi-Electrode switching system. For interpretation, a graphical method is carried out using the two layers curve and the generalized Cagniard graphs (Koefoed 1960) to convert the values of (AB/2) and apparent resistivity values (ρ_a) into an earth model of n-layers having different thicknesses and resistivity. Results of graphical technique were used, as an initial model for IPI2WIN, 2000 software to estimate the final true resistivities and thickness. This program uses a linear filtering approach for the forward calculation (Bobachev et al. 2001) of a wide class of geological models and uses a regularized minimization algorithm using the Tikhonov's approach for the inversion (Gian et al. 2003 and Chuansheng et al. 2008). The quantitative interpretation was used to determine the thicknesses and true resistivities of the stratigraphic units below each VES stations. One VES station (Fig. 3b) was located at borehole (M1) EGSMA (1994) to correlate and calibrate the VES curve parameters (layer resistivity and thickness). The final results of the VES stations were used to construct three geoelectrical cross-sections along Profiles (A–A′, A–B and B–B′) in Fig. 3a.

The geoelectrical cross-section along profile A–A′ (Fig. 4) lies at the upper plateau and includes the VES stations 1, 2, 3 and 4. It exhibits five geoelectrical units belonging to three formations. The first is Maadi Formation which consists of fractured dolomitic limestone of very high resistivity values and it is underlain by a clay unit of 40 m thick and very low resistivity ranging from 1.2 to 4.4 Ωm. The second formation is the Giushi formation, which consists of marly limestone and exhibit moderately high resistivity values ranging from 15 to 48 Ωm and an average thickness of about 60 m. Furthermore, the Mokattam Formation includes two members. The first is the upper building stone member of dolomitic and marblized limestone of high resistivity values ranged from 44 to 210 Ωm and thickness about 40 m; the second is the lower building stone member of marl and marly limestone with very low resistivity ranging from 1.78 to 2.4 Ωm.

The geoelectrical cross-section along profile A–B (Fig. 5), lies at the upper and middle plateaus and it reveals formations different from those of the geoelectrical section A–A′. The geoelectrical cross-section along profile B–B′ (Fig. 6) lies at the middle plateaus and exhibits all formations encountered along A–A′ and A–B profiles. A normal fault F2 was located between VES 6 and 7 with a NW–SE trend and a downthrown in the southwest direction. This fault can be traced at the surface (Fig. 1), its up
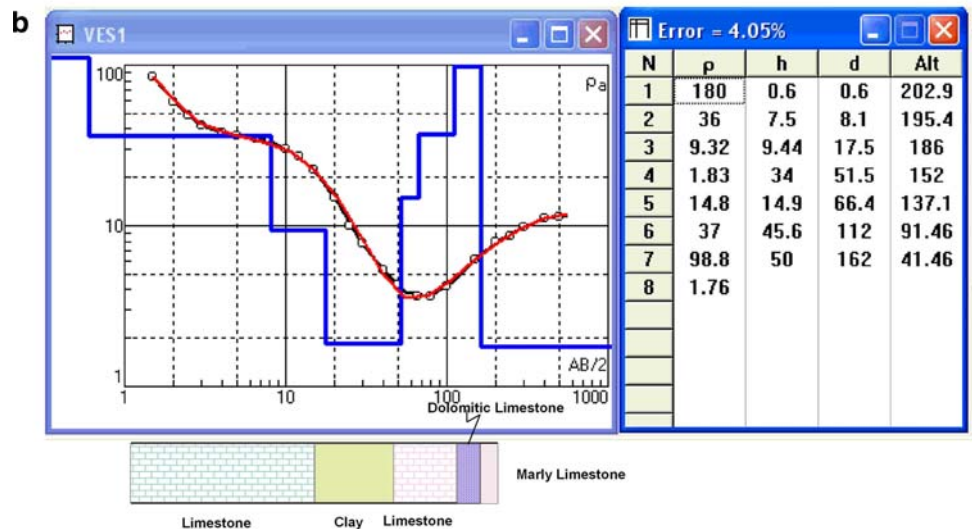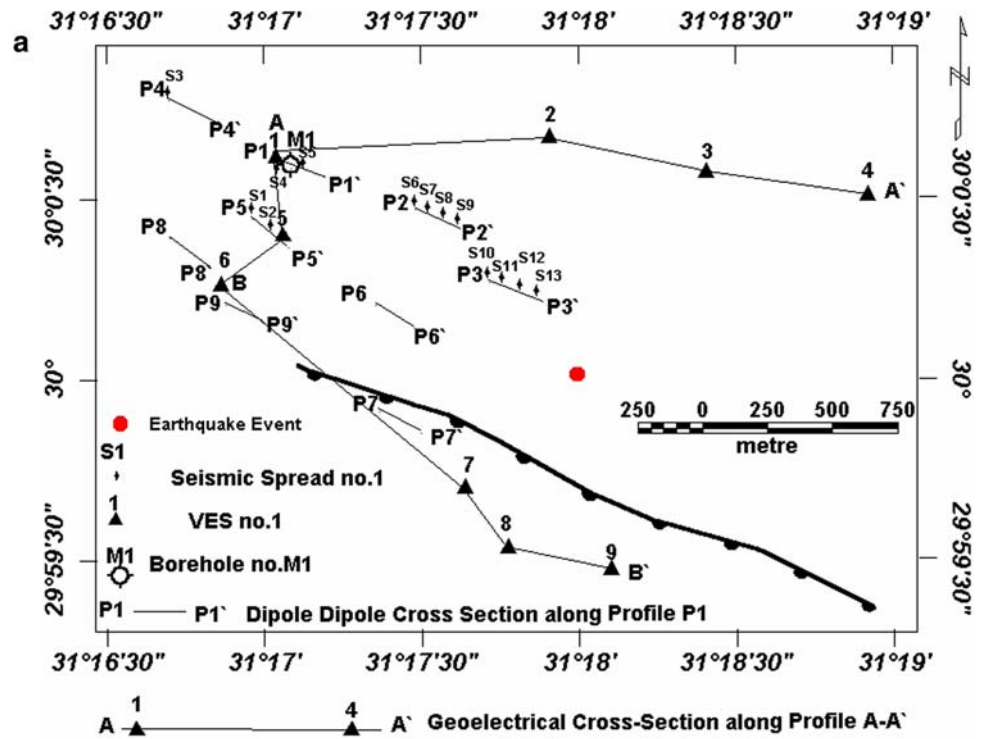
thrown rocks (VES 6) having resistivity values different
from the downthrown rocks (VES 7, 8 and 9).

Shallow geophysical measurements (two-dimensional resistivity and shallow seismic refraction)

Interpretation of dipole–dipole data measurements

Two-dimensional (2-D) electrical imaging surveys are now
widely used in areas with complex geology (Griffiths and

Barker 1993). In the dipole–dipole array, the spacing
between current electrodes (and potential electrodes) are
equal (a). The depth of penetration is a function of (a)
spacing and the dipole separation factor (n). Measurements
were carried out with different (a) values; 5, 10, 15, 20 and
25 m, where dipole–dipole section along profiles 1 and 9
measured by using (a) spacings of 5, 10, 15, 20 and 25 m,
dipole–dipole sections along profiles 2, 5, 7 and 8 mea-
sured by using (a) spacing 5, 10, 15 and 20 m and dipole–
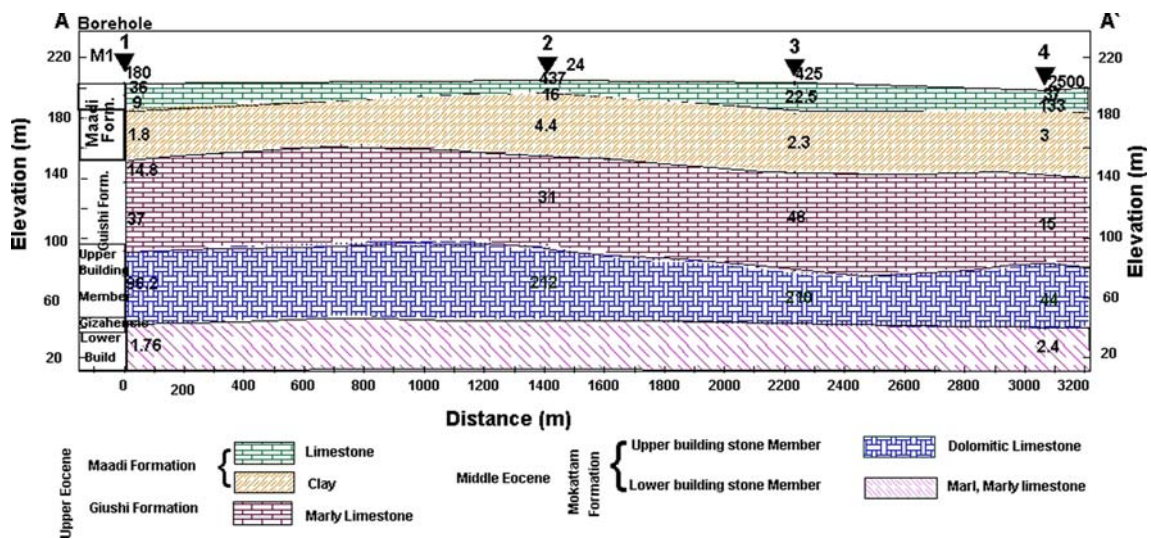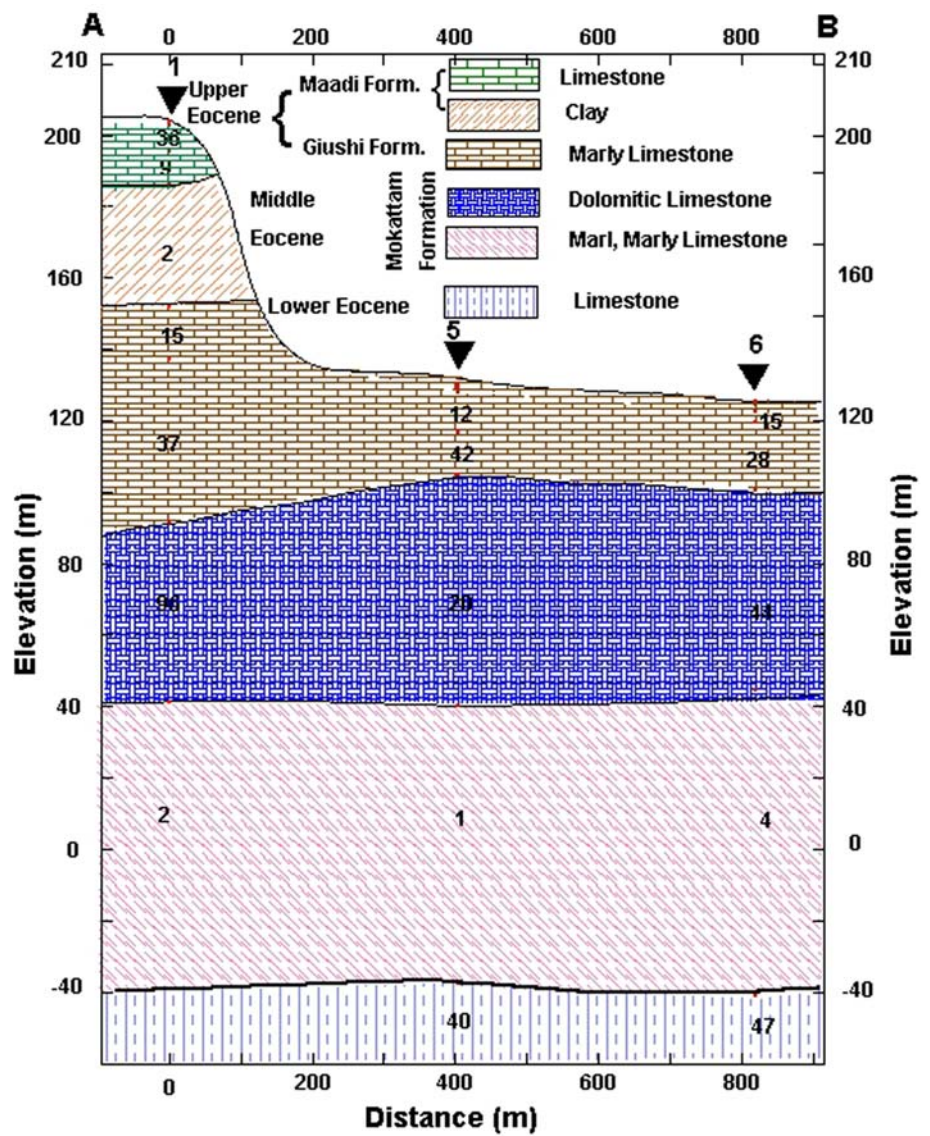dipole sections along profiles 3, 4 and 5 measured by using

Fig. 4 Geoelectrical cross-section along profile A–A′

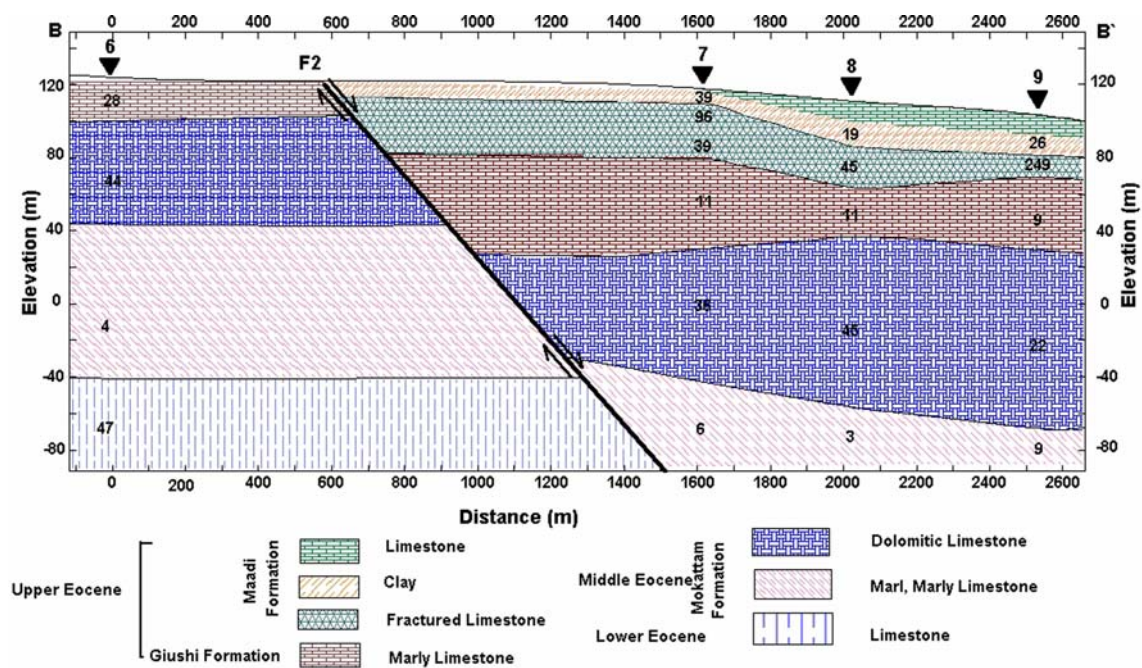**Fig. 5** Geoelectrical cross-section along profile A–B

Fig. 6 Geoelectrical cross-section along profile B–B′

(a) spacing 5, 10 and 15 m. All (a) spacing for all profiles were measured by using (n) factors of 1, 2, 3, 4, 5, 6 and 7. The inversion problem is to find the resistivity of the cells that will minimize the difference between the calculated and measured apparent resistivity values (Loke and Dahlin 2002). The regularized least-squares optimization method with cell-based model is sufficiently flexible to represent almost any subsurface structures with an arbitrarily resistivity distribution (Loke et al. 2003). The processing and interpretation of the obtained data were carried out using the RES2DINV (2003) program, which produced an image of the electrical resistivity distribution in the subsurface based on a regularization algorithm (Loke and Barker 1996). The 2-D inversion model consists of a number of rectangular cells. The arrangement of the cells approximately follows the distribution of the data points in the apparent resistivity pseudosection. In the present study, the obtained data have undergone several processing steps through the RES2DINV software to produce a smooth model. An initial damping factor of 0.16 and minimum damping factor 0.015 were used where the quality of data is good and not too noisy. The width of the interior model cells are the same as the unit electrode spacing.

The dipole–dipole array 2-D surveys were carried out along nine lines as shown in Fig. 3a. These lines are P1–P1′, P2–P2′, P3–P3′, P4–P4′, P5–P5′, P6–P6′, P7–P7′, P8–P8′ and P9–P9′. The dipole–dipole pseudo sections exhibit

large variation of resistivity values corresponding to lateral variation in the subsurface lithological units.

Shallow seismic refraction measurements and interpretation

The seismic spreads were measured close to the geoelectrical dipole–dipole sections. Twenty-four geophones for seismic spreads were used with a spacing of 2–3 m. Three shots are located at distances of −2, 23 and 48 m from the near geophone for a geophone spacing of 2 m. For a geophone spacing of 3 m, the shots were at distances of −3, 43 and 72 m from the near geophone. In this way 12 shallow seismic refraction spreads were measured as shown in Fig. 3a. The seismic spreads nos. 1 and 2 measured at the middle plateau, while the spread nos. 3, 4, 5, 6, 7, 8, 9, 10, 11, 12 and 13 measured at the upper plateau. The shallow seismic refraction surveys were carried out using a seismograph model (StrataView of sensitivity 1 ms) and manufactured by Geometrics, Inc (Yi et al. 2007).

The elastic waves were generated by a 20 kg hammer. The data have been processed and interpreted by using (Sipt2) software package designed by Rimrock Geophysics Inc 1992. The interpretation of data is based on iterative ray-tracing technique, in which the ray propagation will be simulated through a model (Scott 1973).
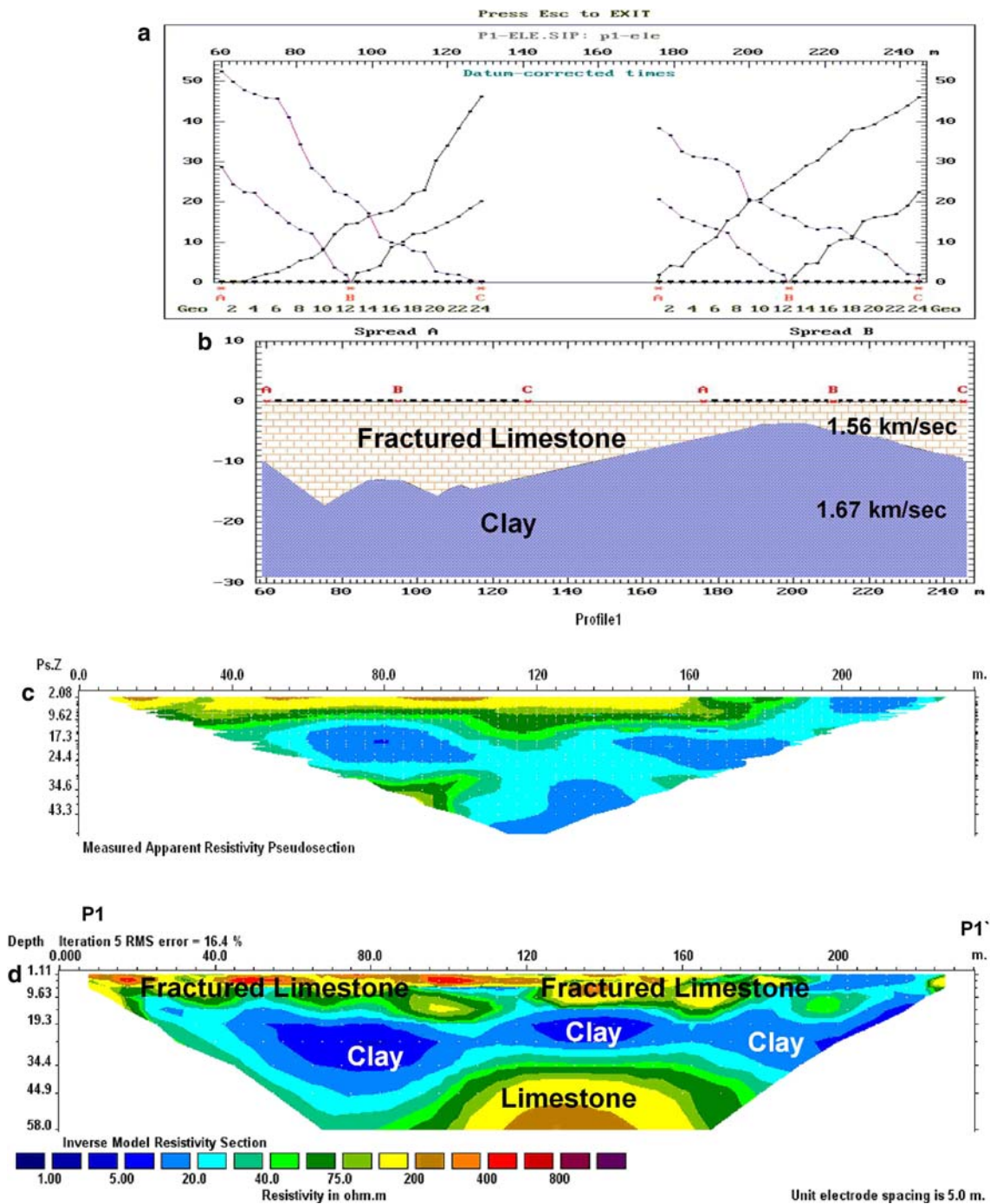
Fig. 7 **a** Time-distance curves, **b** geoseismic section using Sipt2 program, **c** apparent resistivity data, **d** dipole–dipole cross-section along profile P1–P1′

The seismic data of profile 2 (Fig. 8) re-inverting by using seismic refraction tomography program Rayfract software V.3.11 (Schuster and Bosz 1993; Toshiki 1999). The results of inversion for velocity and depth indicated that the velocity values are compatible with the results of Sipt2 program with more details such as occurrence of clay imbedded in limestone layer.

Combined results for dipole–dipole and shallow seismic refraction data

Figures 7, 8, 9 and 10 show results of the interpretation for seismic and dipole–dipole data for the upper plateau. The seismic sections exhibit two layers. The first layer reveals variation in its velocity values ranging from 1.16 to
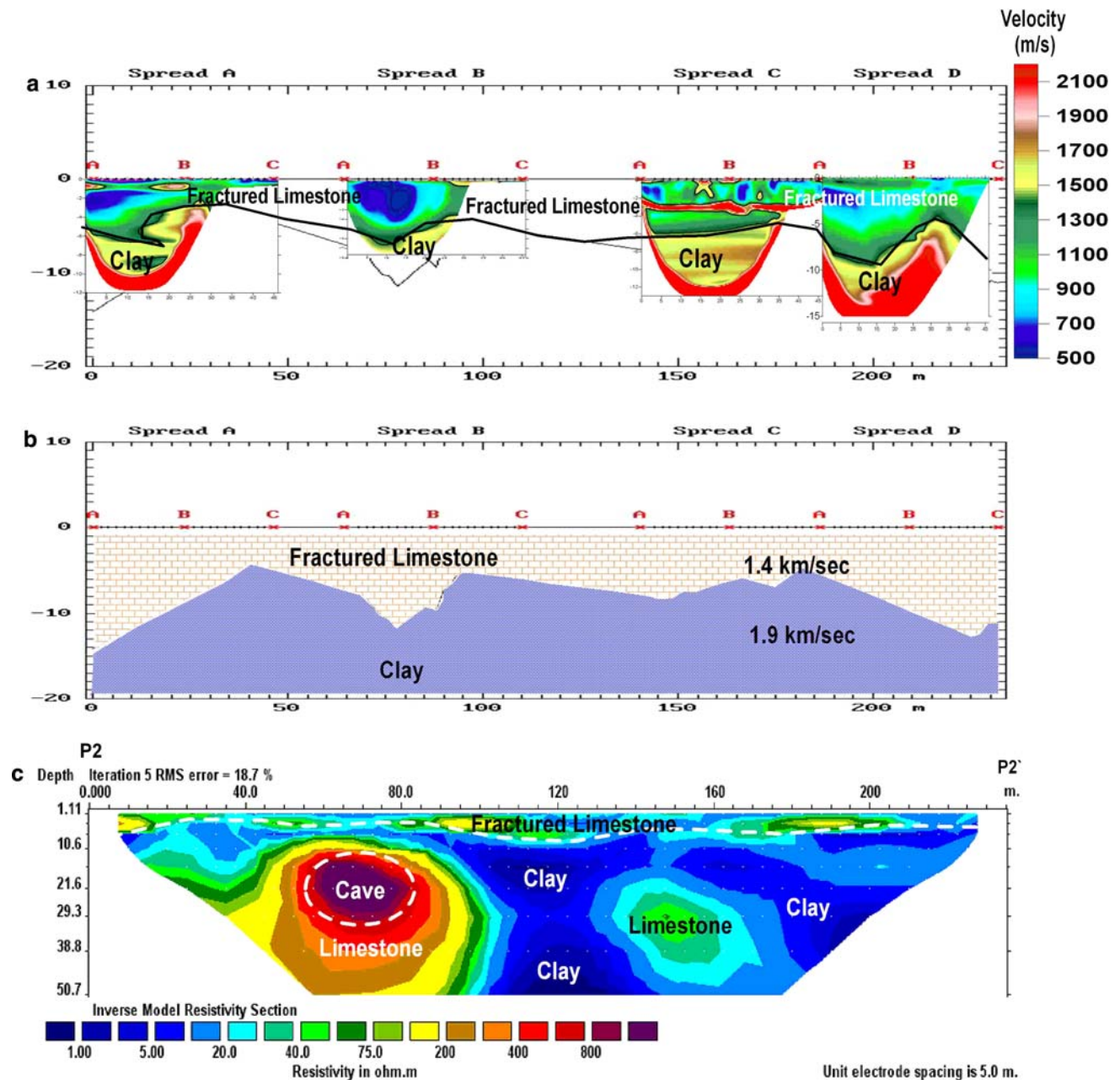
Fig. 8 **a** Geoseismic section using Rayfract seismic tomography program, **b** geoseismic section using Sipt2 program, **c** dipole–dipole cross-section along profile P2–P2′

1.56 km/s. The second layer has velocity values ranging from 1.38 to 2.1 km/s. The dipole resistivity sections reveal large variations in resistivity values. According to such variations, the subsurface section is divided into three layers. The first has high resistivity values and belongs to fractured, dolomitic limestone. The second layer is clay of low resistivity values, and the third layer is limestone of high resistivity values with caves of different dimensions. This formation contains many caves at the northern part of

Mokattam area which are sometimes outcrop at the surface. The profile P5–P5′ located at the middle plateau and the geoseismic section exhibit two layers. The first is marly limestone of low resistivity and with high velocity of 2.1 km/s. The second layer is massive limestone with a velocity of 4.9 km/s (Fig. 11).

The dipole sections along profiles P6–P6′, P8–P8′ and P9–P9′ (Fig. 12) were measured at the middle plateau. They showed variation in the thickness of the marl and the
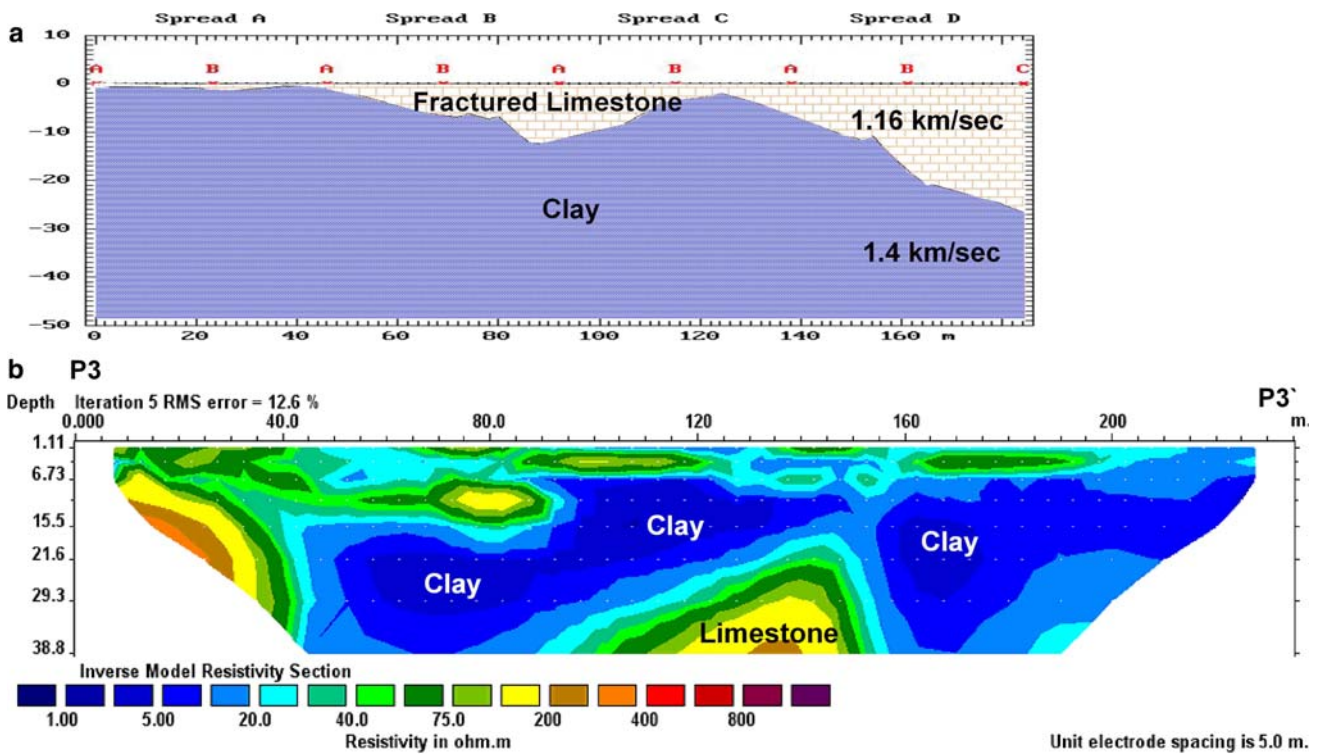
Fig. 9 **a** Geoseismic section, **b** dipole–dipole cross-section along profile P3–P3′
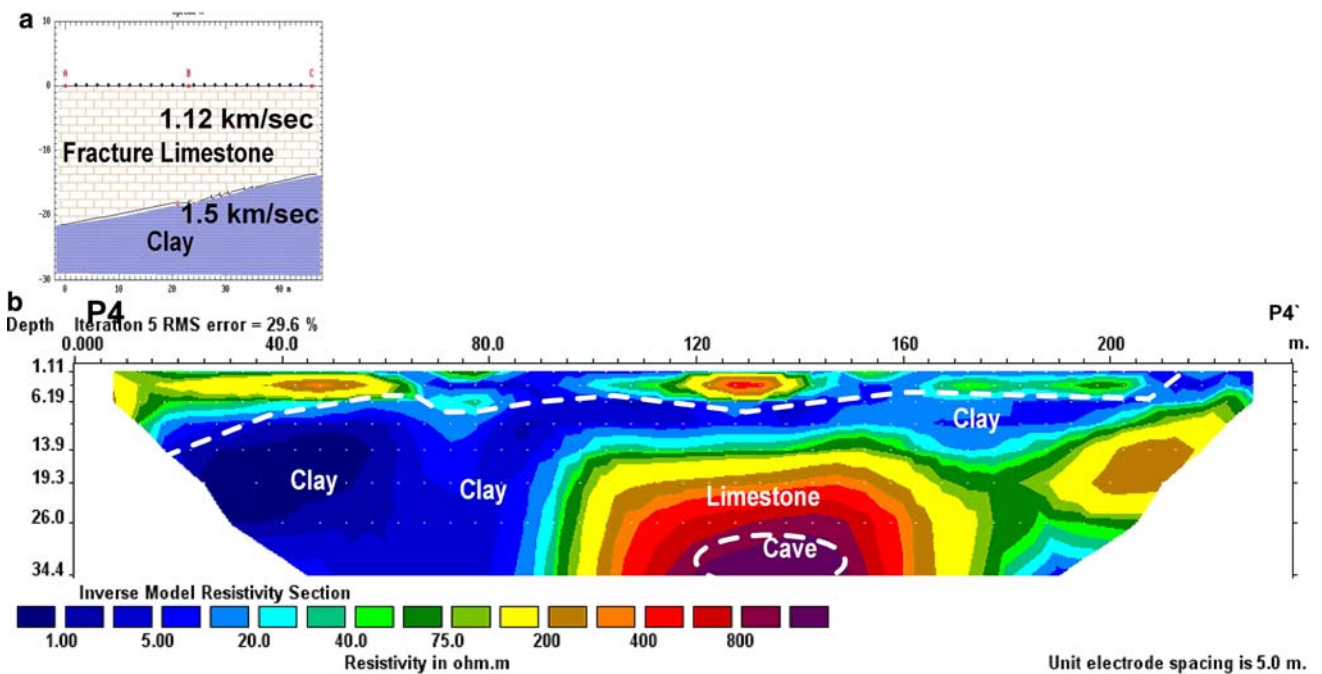

Fig. 10 **a** Geoseismic section, **b** dipole–dipole cross-section along profile P4–P4′
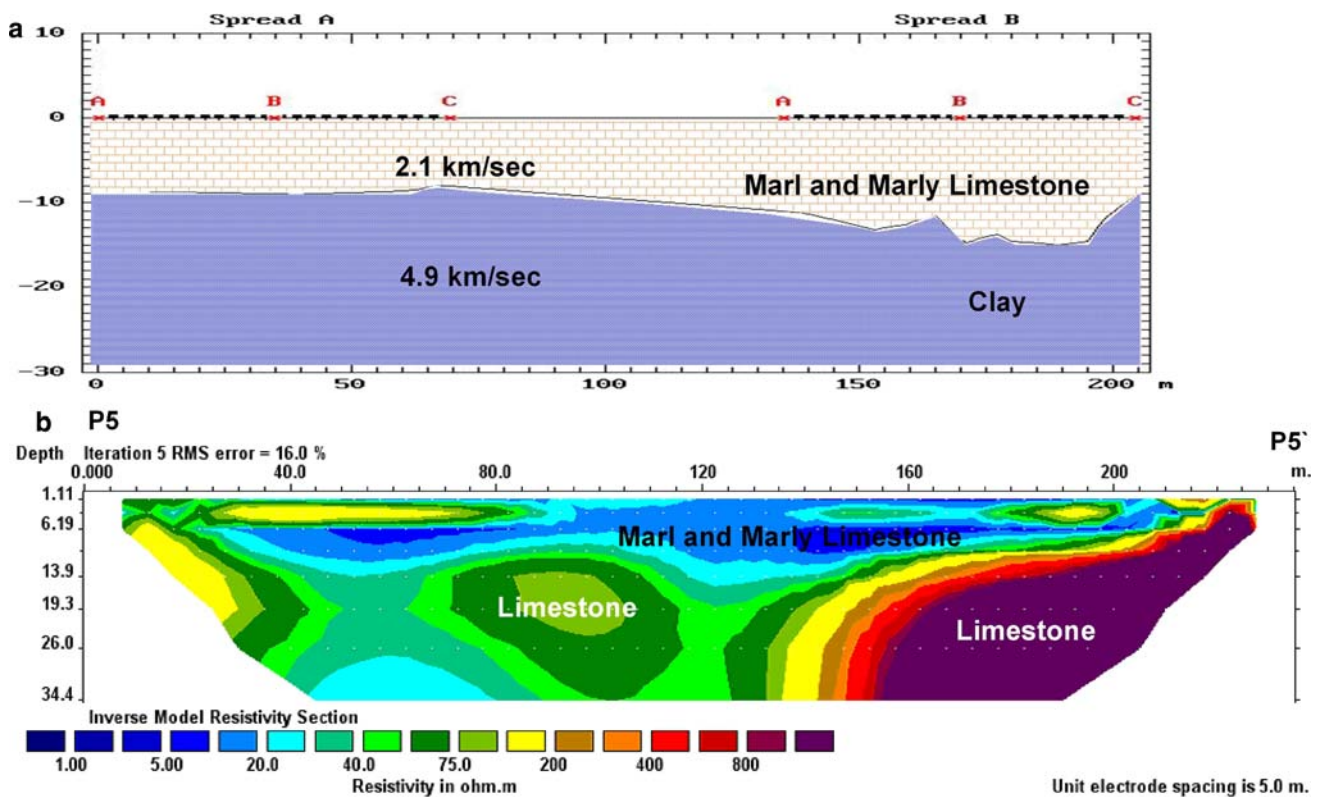
Fig. 11 a Geoseismic section, b dipole–dipole cross-section along profile P5–P5′

limestone. The P7–P7′ profile was measured at the down-thrown of the fault F2 and it exhibits high resistivity for fracture limestone and low resistivity for clay of Maadi formation (Fig. 13).

Seismic activity

Although seismic activity in Egypt is considered low, but seismic risk is considerably high. This is due to the fact, that most of the earthquakes occur close to overpopulated cities and villages, coupled with old methods of construction and poor construction practice. Soil characteristics in different localities in Egypt and their impact on seismic wave attenuation and modification are important parameters that control earthquake risk (El Baz and Reiad 2002). Some earthquake events took place in and around the study area. Table 1 represents 15 earthquake events recorded in and outside the study area through a circle of radius 25 km. The event (9) recorded inside the area of magnitude 3.2 and located near the fault F2, which indicates that fault F2 is an active fault. Therefore, the constructions must be made far away from the fault zone with a distance at least 0.5 km.

Conclusion

This study provided the following conclusions:

1. The subsurface section of the study area consists of different geologic layers belong to different geological ages. The Upper Eocene formations; the first is Maadi Formation consists of fractured limestone and clay, and the second is Giushi Formation that consists of marl and marly limestone. The Middle Eocene Mokattam Formation, which consists of dolomitic limestone, marl and marly limestone. The Lower Eocene Formation is represented by limestone.

2. The shallow part of the upper plateau section consists of fractured limestone with high resistivity and moderate velocity and of thickness of two to five meters. It overlies a clay layer of very low resistivity and moderate velocity. This clay layer may cause some geotechnical problems in the upper plateau due to the hydration. Its thickness is variable and intercalated with fractured limestone.

3. The top layer of limestone in the upper plateau contains caves of different dimensions which may cause some damage to buildings.
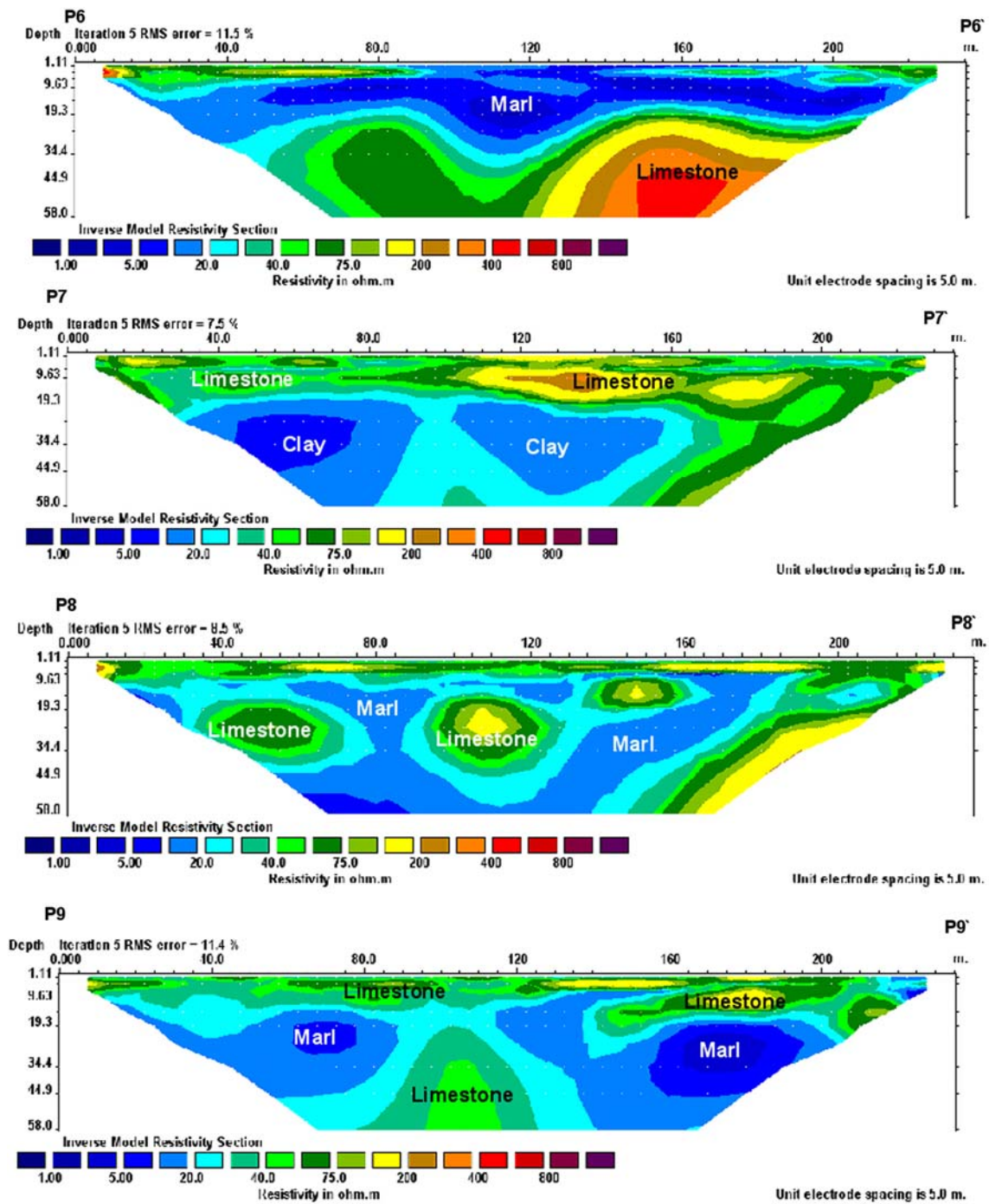
Fig. 12 Dipole–dipole cross-section along profiles P6–P6′, P7–P7′, P8–P8′ and P9–P9′
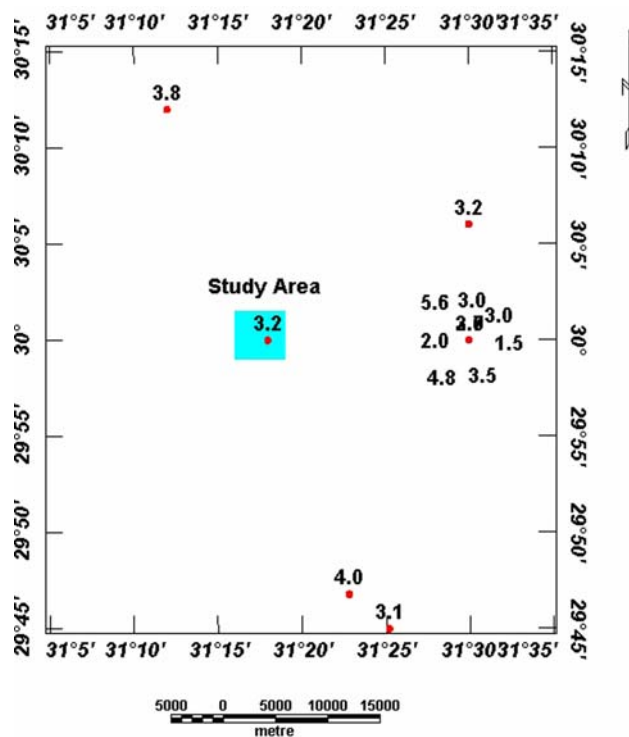
Fig. 13 Distribution of the earthquake events that took place within and around the study area

4. The area is dissected by different fault elements. One of them is an active fault (F2). Planning of a new construction must be far from the fault zone at a suitable distance.

5. Most damages to old constructions may be due to swelling of the clay and the existence of caves in the limestone layer. The middle plateau is a suitable place for new constructions; where the shallow section does not include the clay layer.

References

Bobachev A, Modin I, Shevnin V (2001) IPI2WIN v.2.0, user's manual, Programs set for 1-D VES data interpretation. Department of Geophysics, Geological Faculty, Moscow University, Russia

Chuansheng W, Jinrong H, Xiufen Z (2008) A genetic algorithm approach for selecting Tikhonov regularization parameter. In: IEEE congress on evolutionary computation (CEC 2008)

El Baz F, Riad S (2002) Seismic hazard and seismotectonic of Egypt, Cairo UNESCO Office

Geological Survey of Egypt (EGSMA) (1994) Geological and geophysical studies for Mokattam area, Cairo Government, internal report (in Arabic)

Geological Survey of Egypt (EGSMA) (2004) Geological and geophysical studies for Mokattam area (Phase II), Cairo Government, internal report (in Arabic)

Gian PD, Ernesto B, Cristina M (2003) Inversion of electrical conductivity data with Tikhonov regularization approach: some considerations. Ann Geophys 46(3)

Griffiths DH, Barker RD (1993) Two-dimensional resistivity imaging and modeling in areas of complex geology. J Appl Geophys:29

Koefoed O (1960) A generalized Cagniard graph for interpretation of geoelectric sounding data. Geophys Prospect 8(3):459–469

Loke MH, Barker RD (1996) Rapid least-squares inversion of apparent resistivity pseudosections by a quasi-Newton method. Geophys Prospect 44:131–152

Table 1 Description of the earthquake events that took place within and around the study area

Event no.	Location		Depth (km)	Mag. (Ml)	Date			Time		
	Longitude	Latitude			Day	Month	Year	Second	Minute	Hour
1	31.5	30	20	3	8	8	1934	0	55	8
2	31.5	30	33	5.6	20	7	1954	42	2	5
3	31.5	30	33	4.8	24	7	1954	36	52	0
4	31.5	30	20	3	25	9	1954	39	22	10
5	31.5	30	20	2	11	11	1961	43	30	0
6	31.5	30	20	2	27	10	1962	58	26	7
7	31.5	30	33	3.5	18	10	1964	35	31	18
8	31.5	30	20	1.5	6	1	1965	40	57	11
9	**31.3**	**30**	**20**	**3.2**	**30**	**6**	**1967**	**40**	**41**	**0**
10	31.2	30.2	33	3.8	21	3	1970	23	10	6
11	31.5	30	33	3.5	25	11	1970	1	6	9
12	31.5	30	20	2.7	23	6	1980	2	50	2
13	31.5	30.1	3	3.2	26	3	1986	50	11	12
14	31.38	29.78	18	4	11	6	1999	18.6	52	7
15	31.42	29.75	5	3.1	23	10	1999	0	9	20

Loke MH, Dahlin T (2002) A comparison of the Gauss–Newton and quasi-Newton methods in resistivity imaging inversion. J Appl Geophys 49:149–162

Loke MH, Acworth I, Dahlin T (2003) A comparison of smooth and blocky inversion methods in 2D electrical imaging surveys. Explor Geophys 34:82–187

Moustafa AR, Abdel Twaab S (1985) Morphostructures and non-tectonic of Gabel Mokattam, Middle East Research Center, Ain Shams Uni. Sci Res Ser 5:p68–p78

Moustafa AR, Yehia A, Abdel Twaab S (1985) Structural setting of the area east Cairo, Maadi and Helwan, Middle East Research Center, Ain Shams University. Sci Res Ser 5:40–64

Moustafa AR, El-Nahhas F, Abdel Twaab S (1991) Engineering geology of Mokattam city and vicinity, eastern Greater Cairo, Egypt. Eng Geol 31:327–344

NARSS (1997) Geological and geomorphological studies of the Mokattam plateau, Geological survey of Egypt, Internal Report in Arabic

RES2DINV ver. 3.4 (2003) Rapid 2-D Resistivity & IP inversion using the least-Squares method, Geoelectric Imaging 2-D & 3D, Geotomo software, Malaysia

RIMROCK Geophysics (1992) SIPT2 Refraction Processing Software, Version 3.2, Boulder, Colorado

Schuster GT, Bosz AQ (1993) Wavepath eikonal travel time inversion. Theory Geophys 58:1314–1323

Scott J (1973) Seismic refraction modeling by computer. Geophysics 38(2):271–284

Sultan SA, Helal A, Monteiro Santos FA et al (2004) Geoelectrical application for solving geotechnical problems at two localities in greater Cairo, Egypt. NRIAG J Geophys 3(1):51–64

Sultan SA, Monteiro Santos FA, Helal A (2006) A study of the groundwater seepage at Hibis Temple using geoelectrical data, Kharga Oasis, Egypt. Near Surf Geophys:347–354

Velde B (1995) Composition and mineralogy of clay minerals, origin and mineralogy of clays. Springer, New York, pp 8–42

Toshiki W (1999) Seismic traveltime tomography using Fresnel volume approach. SEG Houston 1999 Meeting, expanded abstracts

Yi MJ, Kim J-H, Song Underwood D (2007) Near-surface seismic refraction surveying field methods, Geometrics, Inc

Yousif MSM (2000) Slope stability of the middle eocene rocks of Gebel Mokattam, ICEHM2000. Cairo University, Egypt, pp 14–22